RSC Advances

ROYAL SOCIETY OF CHEMISTRY

www.rsc.org/advances

Table of contents

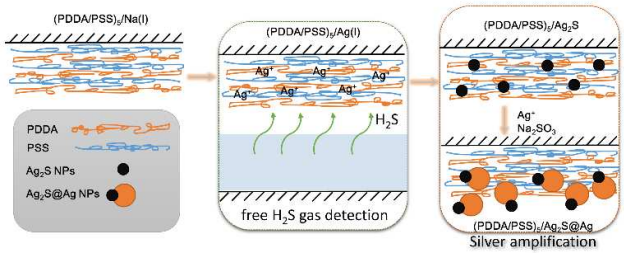

High sensitive and colorimetric detection of hydrogen sulphide by in *situ* formation of Ag_2S@Ag nanoparticles in polyelectrolyte multilayer film

Journal Name

RSCPublishing

COMMUNICATION

High sensitive and colorimetric detection of hydrogen sulphide by in *situ* formation of Ag_2S@Ag nanoparticles in polyelectrolyte multilayer film

Cite this: DOI: 10.1039/xoxxoooooox

Received ooth January 2012,
Accepted ooth January 2012

DOI: 10.1039/xoxxoooooox

www.rsc.org/

Hongxia Fu and Xinrui Duan*

Ag_2S nanoparticles (NPs) was formed by reacting Ag ion with H_2S gas in polyelectrolyte multilayer film. Ag_2S NPs catalyse the formation of Ag NPs later. H_2S (as low as 10 nM Na_2S as donor) was sensitively detected by monitoring the UV-Vis absorbance of newly formed Ag NPs.

H_2S was discovered as one of gas transmitters, along with the other two: nitric oxide and carbon monoxide.[1] H_2S influence cellular events thought regulation of intracellular redox homeostasis and post-translational modification of proteins through S-sulfhydration.[2] H_2S can be endogenously generated by cystathionine beta-synthase (CBS), cystathionine gamma-lyase (CSE), and 3-mercaptopyruvate sulfotransferase, during cysteine metabolism. H_2S mainly is produced by CSE in the cardiovascular system, liver, kidney, and pancreas. More importantly, H_2S level is related to the Down syndrome and Alzheimer's disease.[3]

Many methods have been developed for H_2S detection, including colorimetry,[4] fluorescence technique,[5] electrochemical assay,[6] gas chromatograph,[7] and nanofibers/wires and nanotubes based methods.[8] Recent report shown that hydrogen sulphide concentrations are much lower than presently accepted values in blood and tissues (100 pM in blood and 15 nM in tissues, respectively),[7] to our best knowledge only polarography and gas chromatograph based methods have the ability to detect it, which require involvement of highly toxic mercury and/or complicated instruments. Recent advances of developing fluorescent probes and colorimetry assay[9] have highlighted the need to develop a sensitive, selective, and rapid method for H_2S detection for disease diagnosis and in *vitro* cultured cell based inhibitor screening for H_2S related enzymes. Up to date, Lack of affordable and sensitive method still is the major obstacle for such applications.

In this work, we would like to develop a sensitive, selective, and rapid method for H_2S detection based on Ag_2S NPs catalysed formation of Ag NPs in layer-by-layer polyelectrolyte multilayer film. Ag_2S NPs itself have been employed in colorimetric H_2S sensing.[4b] With common microplate reader, the limit of detection is 8.7 μM. Formation of Ag_2S on metallic silver probe caused light reflection difference could detect as low as 100 nM of H_2S.[4c] By using Au@Ag NPs and sophisticated dark-field microscopy, as low as 50 nM of H_2S can be detected.[4d]

Su and his co-workers extensively studied in *situ* formation of Ag NPs in layer-by layer polyelectrolyte multilayer film (PEMs).[10] Shannon and his co-workers have prepared Au/CuI and Au/CdS core-shell nanoparticle in poly (diallyl dimethylammonium)(PDDA) by using electrochemical atomic layer deposition[11]. Li and his co-workers have prepared CuS NPs in PVA polymer matrix in by embedded copper ion with H_2S gas.[12] Under the inspiration of these previous works and the fact of PEMs are very stable in aqueous solution, we designed our system as follow:

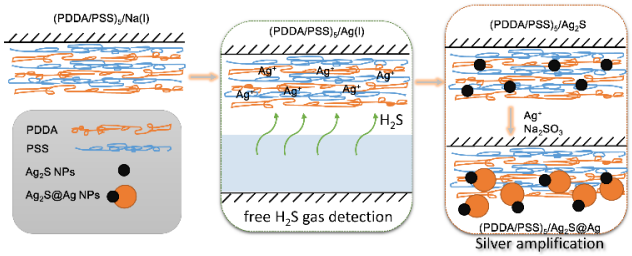

Scheme 1. Mechanism of H_2S gas detection.

As shown in **Scheme 1**, PEMs was prepared by standard layer-by-layer process in the present of extra sodium ions. Sodium ions were exchanged with Ag ions later. At physiological pH, the assay takes advantage of the volatility of H_2S gas. As H_2S is volatilized in a microplate well, it can react with the Ag ion to form Ag_2S NPs. Ag NPs can be generated on Ag_2S NPs by reducing Ag^+ ions with hydroquinone or sodium sulphite in solution.[13] UV Light irradiation substantially accelerate this process. Because of this catalysis effect of Ag_2S NPs, Ag NPs were formed at Ag_2S NPs site in the PEMs in the presence of silver nitrate and Na_2SO_3, which greatly improved the sensitivity of detection. Concentration of silver nitrate and sodium sulphite, and time of amplification have great impact on the silver amplification process, thus we chosen the previous reported optimized the concentrations for our study. Furthermore, we optimized the time of amplification (Figure S2). Two hours of amplification have the best signal/noise ratio.

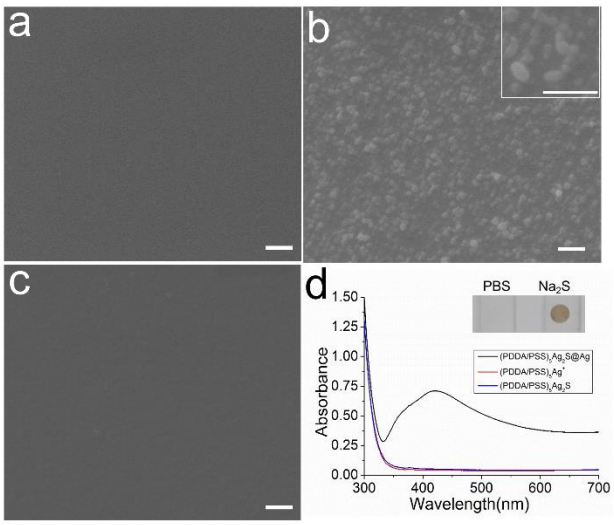

Figure 1. SEM images of (a) $(PDDA/PSS)_5/Ag(I)$, (b) $(PDDA/PSS)_5/Ag_2S@Ag$, and (c) $(PDDA/PSS)_5/Ag_2S$. (d) UV-Vis spectra of all films and insert is the image of PEM films on top of PBS solution or Na_2S solution after silver amplification. 10 μM Na_2S solution was used to generate all PEM films for SEM imaging and UV-Vis Spectra. Magnification of all SEM images is 50,000x, except insert image of Figure 1b that is 100,000x. Scale bar = 500 nm.

We use Na_2S as the H_2S donor to develop our detection method, since the purity (>98%) is much higher than commercially available NaSH, which may contain polysulfides and have a purity of only 60%.[14] H_2S gas spontaneously release from Na_2S aqueous solution until the HS^- and S^{2-} are used up. H_2S react with the Ag ions embedded in $(PDDA/PSS)_5$ film coated on the glass slide. After it reacts with H_2S gas from the Na_2S solution and Ag_2S NPs formed in the nano-size space of PEMs.[10a] Scanning electron microscopy (SEM) images and the absorption spectra of $(PDDA/PSS)_5/Ag^+$, $(PDDA/PSS)_5/Ag_2S$, $(PDDA/PSS)_5/Ag_2S@Ag$ PEMs are shown in **Figure 1**. Magnification of all SEM images is 50,000x, except insert image of Figure 1b that is 100,000x. $(PDDA/PSS)_5/Ag^+$ film does not have any significant morphology under SEM and has a weak absorption in the corresponding wavelength region due to absorption of glass.

Although formed Ag_2S NPs can be barely seen under SEM, we could observe roughness increase of $(PDDA/PSS)_5/Ag_2S$ film (**Figure 1c**). And it does produce broad absorption band in UV-Vis spectra (Figure S1, UV-Vis spectra of high concentration of Ag_2S NPs). Although SEM is not the ideal tool for characterization of Ag_2S NPs morphology, but existence of silver NPs after silver amplification also support the existence of former formed Ag_2S NPs. Ag amplification has been extensively studied where silver ions were reduced to metallic silver in the presence of a reducing agent (such as Na_2SO_3).[13] Previous work reported the catalysis effect of Ag_2S NPs in solution, in our work we also observed this phenomenon in PEMs film. After silver amplification process Ag NPs appear clearly under SEM (**Figure 1b**). As for the UV-vis detection in **Figure 1d**, a much stronger absorption peak appears around 430 nm after silver amplification. Insert image is the image of PEM films took by cell phone camera were on top of PBS solution or Na_2S solution in 96 well plate after silver amplification. We can see the circular shape of the spot that are well preserved the shape of a well. By converting absorption signal of Ag_2S NPs to Ag NPs in PEMs, The sensitivity of H_2S detection was greatly improved due to following reasons: 1) Maximum absorption peak of Ag NPs are higher than 300 nm that avoid the inference of glass slide and cell culture plate itself; 2) Ag_2S NPs serves as catalyst that will result in significant signal amplification.

To get direct view of the morphology and the composition of $Ag_2S@Ag$ NPs in PEM films, we studied the sample with field emission transmission electron microscopy (FE-TEM) under scanning TEM (STEM) mode and energy dispersive X-ray analysis (EDX) under STEM of single particle in PEM films, results are shown

in **Figure 2**. Since the NPs are crowded in high concentration samples (as shown in **Figure 1b**), we chosen the sample from lower concentration of H_2S (500 nM) for all the STEM study. PEM film was prepared by scratching it off from glass surface in water. And the film was floating on the water surface and later was caught by a TEM copper grid.

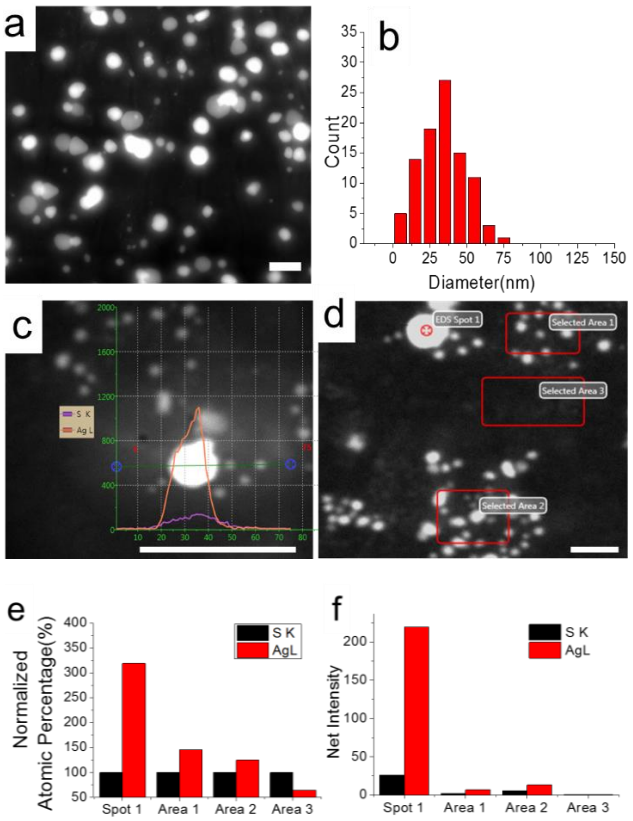

Figure 2 (a) STEM image of NPs. (b) size distribution of NPs. (c) Line scan of STEM-EDX analysis of silver and sulphur content of single NP. (d) Spot and area analysis of silver and sulphur content by STEM-EDX. Scale bar = 100 nm. 500 nM Na_2S solution was used to generate PEM film for STEM imaging and EDX analysis.

Figure 2a shows the morphology of single NPs under FE-TEM by using STEM mode. Size distribution of NPs are shown in **Figure 2b**. Majority of particles have the diameter between 20 to 70 nm. It is worthy to notice, beside large and bright particles, some very small particles with the diameter of several nanometers can be seen surrounding bigger particles. It is more clearly with higher magnification image in **Figure 2c**. We assume that the smaller particles are Ag_2S NPs and the bigger particles are Ag NPs that newly formed on Ag_2S NPs site. We did the line scan of STEM-EDX analysis to find out the content difference in two kinds of particles. As shown in **Figure 2c**, net intensity of silver content is much higher than sulphur content on the bigger NP. Since the intensity of single small particle is too weak, we performed area analysis on crowded area of small particles to get more comparable results with spot from bigger particle. Selection of area and spot are shown in **Figure 2d**. Normalized atomic percentage and net intensities are shown in **Figure 2e** and **f** respectively. The atomic ratio of silver and sulphur in the 20 nm particle is around 3.2 that confirmed the formation of Ag_2S@Ag NPs. The atomic ratio of particles with the diameter of several nanometers is around 1.5 that is very close to the theoretical ratio of Ag_2S. This difference of ratio in between our observation and theoretical ratio might due to the low net intensity of area 1 and area 2 that will cause the increase of error. Area 3 was selected to show the background signals, from the **Figure2f**, we can see the background signals are neglectable. Spectra of EDX analysis are represented in **Figure S3**.

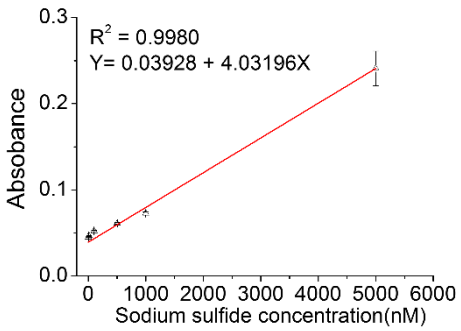

Figure 3. Standard curve of H_2S detection (from 10nM to 5000nM) by measuring absorbance of $(PDDA/PSS)_5/Ag_2S$@Ag. Error bars represent standard deviation (n=3). H_2S gas from Na_2S solution was used to react with $(PDDA/PSS)_5/Ag^+$ to generate $(PDDA/PSS)_5/Ag_2S$, which further treated with mixture of $AgNO_3$ and Na_2SO_3 solution to generate $(PDDA/PSS)_5/Ag_2S$@Ag.

Figure 3 shows standard curve of various concentrations (from 10 nM to 5 μM) of Na_2S solutions with Ag_2S@Ag NPs absorbance. Good linear relationship between the UV absorption at 430 nm and the concentration of Na_2S solution (10nM-5μM) was observed. Linearity equation is $A = 0.03928+4.03196C$. R square is 0.9980.

To test the specificity of our method, biologically relevant molecules include reactive sulfur such as dithiothreitol (DTT), cysteine (CYS), and reduced glutathione (GSH) as well as cell culture medium, DMEM and DMEM plus 10% fetal bovine serum (FBS) were studied. As shown in **Figure 4a**, under same reaction conditions, all interfere candidates with a 2000 fold higher concentration of Na_2S only produce same UV absorption intensity with control (PBS buffer solution). These results demonstrate excellent selectivity of our method for H_2S gas detection. This high selectivity of our method is similar with previous reported hydrogen sulphide gas based detection

methods,[4b, 5d] which is interfere candidates only produce comparable signals with control solution.

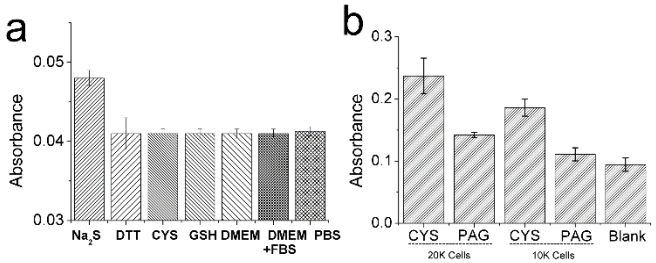

Figure 4. (a) Effect of possible interference on H_2S detection. DTT, CYS, GSH, DMEM, and DMEM plus 10% FBS. PBS solution was used as control. The concentration of these substances are all 200 μM except Na_2S is 100 nM. Error bars represent standard deviation (n=3). (b) Measurement of free H_2S gas generated from live HepG2 cells. Error bars represent standard deviation (n=3).

With the excellent sensitivity and selectivity of our method, we are confident to perform the detection of cellular endogenous H_2S gas. Since H_2S mainly is produced by CSE in the liver, cardiovascular system, kidney, and pancreas. Liver cancer cell line HepG2 was used in this section of study. Before detection cells are pre-treated with cysteine (CYS) and pyridoxal phosphate (PLP) to generate H_2S gas. Blanks are same treatment without cells. CSE inhibitor propargylglycine (PAG) was added to proof the inhibitor monitoring ability of our method in live cells.[3] PEMs coated glass slides were glued on 96 well plate cover and placed on top of well plate for 2 hours and after 2 hours silver amplification process resulting glass slides were measured by microplate reader. As shown in **Figure 4b**, 1 x 10^4 (10K) cells (e.g. about 30% coverage of 0.32 cm^2 area) can be detected in a 96 well plate format, and 2 x 10^4 (20K) cells produce higher signal than 10K cells. Since we use same amount of PAG, absorbance of the PAG added sample of 20K cells also lightly increased. Signals from cells are significant higher than blank and PAG treated samples.

Previous report on free H_2S gas detection of live cells is based on zinc salts embedded in Agar hydrogel.[5a] After 12 hours or longer incubation, acid were added to release H_2S gas from formed ZnS precipitation and released H_2S gas reacted with *N*,*N*-dimethyl-p-phenylenediamine chloride and $FeCl_3$ to produce Methylene blue. Measuring absorbance of the produced methylene blue will give quantity of H_2S gas. Our method holds two significant improvements: 1) High sensitivity of our method makes the incubation time is shorten from 12 hours to 2 hours; 2) in *situ* formation and silver amplification ensure reacted spots were well preserved, so results can be readily obtained by using micro-plate reader.

We thank the National Natural Science Foundation of China (Grant No. 21305083) and Fundamental Research Funds for the Central Universities (Grant No. GK201303003 and GK201402051) for financial support.

Conclusions

We reported a sensitive, selective, and rapid colorimetric method for cellular endogenous H_2S gas detection based on in *situ* formation of Ag_2S@Ag NPs in layer-by-layer PEMs. When use Na_2S solution as gas source, H_2S from 10 nM (3 picomole, calculated by sulfur element) of 300 μL Na_2S solution in pH 7.0 buffer solution can be detected effectively. As far as we know, this method is the most sensitive among colorimetric method and has comparable sensitivity with the most sensitive polarographic and gas chromatographic approaches. And our method only required a microplate reader with UV-Vis absorbance detecting ability for detection. Reaction between H_2S and silver ion generated Ag_2S NPs that catalyse rapid formation of Ag NPs on Ag_2S NPs surface, thus absorption intensity of Ag_2S NPs was transferred to absorbance of newly formed Ag NPs. That results in signal amplification and high sensitivity. Since our method was designed to only measure H_2S gas, potential interfere including common thiols and standard DMEM medium plus 10% FBS does not affect detection. Due to excellent sensitivity and selectivity, we believe our method is significantly important for disease diagnosis and in vitro cultured cell based inhibitor screening for H_2S related enzymes.

Notes and references

[a] Key laboratory of analytical chemistry for life science of Shaanxi Province, School of Chemistry and Chemical Engineering, Shaanxi Normal University, Xi'an, Shaanxi, 710119, P. R. China. E-mail: duanxr@snnu.edu.cn

† Electronic Supplementary Information (ESI) available: [Experimental details and UV-Vis spectra of $(PDDA/PSS)_5/Ag_2S$ form under high concentration of Na_2S, effect of silver amplification time, spectra of EDX analysis are presented in Electronic Supporting Information.]. See DOI: 10.1039/c000000x/

1 R. Wang, *Curr. Opin. Nephrol. Hy.* 2011, **20**, 107-112.

2 (a) J. Pan, K. S. Carroll, *Biopolymers* 2013, **101**, 165-172. (b) *J. Yang, V. Gupta, K. S. Carroll and D. C. Liebler, Nat. Commun*. 2014, **5,** 4776.

3 (a) M. Thorson, T. Majtan, J. Kraus, A. Barrios, *Angew. Chem. Int. Ed.* 2013, **52**, 4641-4644. (b) H. Peng, Y. Cheng, C. Dai, A. King, B. Predmore, D. Lefer, B. Wang, *Angew. Chem. Int. Ed.* 2011, **50**, 9672-9675.

4 (a) R. Kartha, J. Zhou, L. Hovde, B. Cheung, H. Schröder, *Anal. Biochem.* 2012, **423**, 102-108. (b) A. Jarosz, T. Yep, B. Mutus, *Anal. Chem.* 2013, **85**, 3638-3643. (c) H. Kong, Z. Ma, S. Wang, X. Gong, S. Zhang, and

X. Zhang, *Anal. Chem.* 2014, **86**, 7734−7739. (d) J. Hao, B. Xiong, X. Cheng, Y. He, E. Yeung, *Anal. Chem.* 2014, **86**, 4663-4667.

5 (a) Y. Qian, J. Karpus, O. Kabil, S.Y. Zhang, H. L. Zhu, R. Banerjee, J. Zhao, C. He, *Nat. Comm.*, 2011, **2**, 495; (b) A.R. Lippert, E. J. New, C. J. Chang, *J. Am. Chem. Soc.*, 2011, **133**, 10078-10080. (c) Y. Chen, C. Zhu, Z. Yang, J. Chen, Y. He, Y. Jiao, W. He, L. Qiu, J. Cen, Z. Guo, *Angew. Chem. Int. Ed.* 2013, **52**, 1688-1691. (d) A. Faccenda, J. Wang, B. Mutus, *Anal. Chem.* 2012, **84**, 5243-5249. (e) Y. Zhou, J. Yu, X. Lei, J. Wu, Q. Niu, Y. Zhang, H. Liu, P. Christen, H. Gehring, F. Wu, *Chem. Commun*. 2013, **49**, 11782-11784.

6 (a) G. Schiavon, G. Zotti, R. Toniolo, G. Bontempelli, *Anal. Chem.*1995, **67**, 318-323. (b) J. Doeller, T. Isbell, G. Benavides, J. Koenitzer, H. Patel, R. Patel, J. Lancaster, V. Darley-Usmar, D. Kraus, *Anal. Biochem.* 2005, **341**, 40-51.

7 (a) J. Furne, A. Saeed, M. D. Levitt, *Am. J. Physiol. Regul. Integr. Comp. Physiol.* **2008**, 295, R1479.

8 (a) W. Zheng, X. Lu, W. Wang, Z. Li, H. Zhang, Z. Wang, X. Xu, S. Li, C. Wang, *J. Colloid Interface Sci.* 2009, **338**, 366-370. (b) L. Ji, A. Medford, X. Zhang, *Polymer* 2009, **50**, 605-612. (c) L. Mai, L. Xu, Q. Gao, C. Han, B. Hu, Y. Pi, *Nano Lett.* 2010**, 10**, 2604-2608. (d) S. Mubeen, T. Zhang, N. Chartuprayoon, Y. Rheem, A. Mulchandani, N. Myung, M. Deshusses, *Anal. Chem.* 2010, **82**, 250-257.

9 (a) J. Zhang, Y. Q Sun, J. Liu, Y. Shi, W. Gou, *Chem. Commun.* 2013, **49**, 11305-11307. (b) F. Yu, X. Han, L. Chen. *Chem. Commun.*, 2014, **50**, 12234-12249. (c) Z. Huang, S. Ding, D. Yu, F. Huang, G. Feng, *Chem. Commun.,* 2014, **50**, 9185-9187. (d) T. Ozdemir, F. Sozmen, S. Mamur, T. Tekinay, and E. U. Akkaya, *Chem. Commun.*, 2014, **50**, 5455-5457. (e) Y. Zhou, J. Yu, X. Lei, J. Wu, Q. Niu, Y. Zhang, H. Liu, P. Christen, H. Gehringe and F. Wu, *Chem. Commun.*, 2013, **49**, 11782--11784

10 (a) X. Zan, Z. Su, *Langmuir* 2009, **25**, 12355-12360.; (b) J. Wei, L. Wang, X. Zhang, X. Ma, H. Wang, Z. Su, *Langmuir* 2013, **29**, 11413-11419.; (c) X. Zan, M. Kozlov, T. McCarthy, Z. Su, *Biomacromolecules* 2010, **11**, 1082-1088.

11 (a) C. Gua, H. Xua, M. Parka, C. Shannona, *ECS Trans.,* 2008, **16**, 181-190. (b) C. Gu, Hui, M. Park, C. Shannon, *Langmuir* 2009, **25**, 410-414

12 J. Xu, X. Cui, J. Zhang, H. Liang, H. Wang, J. Li, *Bull. Mater. Sci.* 2008, **31**, 189-192.

13 (a) A. Kryukov, A. Stroyuk, N. Zin'chuk, A. Korzhak, S. Kuchmii, 2004, **221**, 209-221. (b) M. Pang, J. Hu, H. Zeng, *J. Am. Chem. Soc.* 2010, **132**, 10771-10785.

14 M. Whiteman, S. Trionnaire, M. Chopra, B. Fox, J. Whatmore, *Clin. Sci.* 2011, **121**, 459-488.